Regular Article

Characterization of Tableting Speed-Dependent Deformation Properties of Active Pharmaceutical Ingredients in Powder Mixtures Using Out-of-Die Method

Daisuke Mizunaga,*[a,b] Mika Koseki,[a] Naoki Kamemoto,[a] and Satoru Watano[b]

[a] *Formulation Research Institute, Otsuka Pharmaceutical Co., Ltd.; 224–18 Ebisuno, Hiraishi, Kawauchi-cho, Tokushima 771–0182, Japan: and* [b] *Department of Chemical Engineering, Osaka Prefecture University; 1–1 Gakuen-cho, Naka-ku, Sakai, Osaka 599–8531, Japan.*

Received August 8, 2021; accepted September 22, 2021

A quantitative evaluation method for determining the effect of tableting speed on the compression properties of pharmaceutical powders was investigated in this study. Cilostazol and ibuprofen were used as active pharmaceutical ingredients (APIs) and mixed with lactose monohydrate and microcrystalline cellulose. Viscoelasticity was examined to evaluate the raw material, and stress relaxation tests were conducted to determine the apparent viscosity and elasticity coefficients of the placebo and two APIs. Tablets were prepared using a compaction simulator and a rotary tablet press at the tableting speeds ranging from laboratory to commercial. The in-die or out-of-die strain rate sensitivity (SRS) indices were determined as a measure of the compressibility and compactibility. The results showed that the sensitivity of the out-of-die SRS was higher than that of the in-die SRS. The out-of-die SRS of ibuprofen 20% powder, which showed high elasticity and low viscosity, was 13.3–47.9%, whereas that of the placebo and cilostazol 20% (w/w) powder was <7.5%. A peripheral speed difference of more than 300 mm/s during the out-of-die SRS was sensitive enough to detect the capping tendency. Cilostazol, which has lower elasticity and higher viscosity than ibuprofen, was tested using powder mixtures with the API concentrations of 5–40%; the compressibility SRS was <5% for all API concentrations. In contrast, the compressibility SRS of ibuprofen increased from 4.8 to 81% depending on the API concentration. Using the compressibility SRS as an index, it was possible to extract the tableting speed-dependent compressibility characteristics of API from the powder mixtures containing API.

Key words tableting speed; strain rate sensitivity; out-of-die; compression; viscoelasticity; scale-up

Introduction

Tablets are the most common dosage form among pharmaceutical products and are manufactured by compacting a mixture of raw materials or granules in a rotary tablet press. The tableting process is a necessary process that affects the product quality characteristics such as appearance, dissolution of active pharmaceutical ingredients (API), and stability. It also adds physical strength to the powder for the transport to the following process, such as film coating and packaging. However, problems with the compressibility of powder and the manufacturing conditions can cause tableting defects. Capping is a tablet failure, in which the tablet surface peels off in a cap shape, and if it occurs during the process, the manufacturing should be stopped. In contrast, even if the tablet is ejected from a rotary tablet press, there are cases where it is damaged during the transport or the film-coating steps. The mechanism of capping is related to several factors, such as the powder properties and the manufacturing conditions. For example, the powder properties related to the occurrence of capping, stress relaxation,[1,2] elastic recovery,[3] and residual die-wall pressure have been reported.[4,5] In particular, high-pressure compaction and high tableting speeds are more susceptible to these effects. Air entrapment during the powder compaction and other factors can also cause the capping.[6,7]

The compression mechanism differs between a single-punch tablet press and a rotary tablet press. Additionally, during the tableting process using a rotary tablet press, increasing the tableting speed (reducing the compression time/dwell time) for scale-up becomes an issue because in the commercial-scale rotary tablet press,[8] the number of punches and dies used increases the production capacity. As a result, the turret becomes more extensive; therefore, even at the same turret rotation speed, the compression time is significantly reduced because of the higher peripheral speed. It is challenging to predict the commercial-scale tableting conditions using a laboratory-scale rotary tablet press. Therefore, it is important to bridge the differences between mechanical and geometrical factors and detect tableting issues during the early formulation development stage. To achieve this, it is necessary to understand the compression properties and establish a method for evaluating the increased tableting speed for scale-up.

Compression properties are related to a combination of material properties of the raw material, such as elasticity/viscoelasticity, plasticity/viscoplasticity, brittleness, and ductility.[9–13] Tests for evaluating the compression properties include rheological tests such as stress relaxation tests and creep tests or compressive energy evaluation methods based on the displacement-force curve in the compression.

Stress relaxation is a phenomenon in which the stress decreases over time when constant stress/strain is applied. By mathematically analyzing the stress decay curve obtained from the time variation of stress, parameters related to the viscoelasticity of the raw material can be obtained.[14] In contrast, at the point of maximum compression, viscoelasticity and viscoplasticity occur at the compression peak.[10] Although the parameters obtained from stress relaxation tests do not

* To whom correspondence should be addressed. e-mail: Mizunaga.Daisuke@otsuka.jp

represent only viscoelasticity, this approach helps classify the raw material properties using a simple evaluation method to determine the apparent viscoelasticity. The relevance of this method to capping properties has also been reported.[1)]

Heckel analysis is used to evaluate deformation characteristics related to the compression.[15)] This method is based on the response of powder porosity to pressure during compaction. The reciprocal slope of the linear part of the Heckel plot represents the mean yield pressure, which is an index of plastic deformation.[16)] Heckel analysis is also known as the in-die method ("at-pressure method")[2,17–19)] and out-of-die method ("zero-pressure method").[20,21)] The in-die method requires a sensor to measure the punch displacement and compression force simultaneously, and it is essential to accurately measure the height of the powder bed in the die. Elastic deformation of the equipment must also be considered during compaction. Hirschberg *et al.* used four pharmaceutical excipients (microcrystalline cellulose, α-lactose monohydrate, starch, and dibasic calcium phosphate dihydrate) as samples and divided the elastic recovery of the tablet into three components (in-die axial, out-of-die axial, and radial).[22)] They showed that the in-die elastic recovery (ER_{in}) was linearly dependent on the compression pressure at the time of examination, whereas the out-of-die elastic recovery (ER_{out}) was a material constant. Katz and Buckner proposed a method for generating accurate compressibility and compactibility profiles from in-die data of tablets manufactured at two levels of compression pressure and from changes in the solid fraction of ejected tablets.[21)]

Strain rate sensitivity (SRS) is used to evaluate the rate-dependent compression behavior of powders from Heckel analysis at two tableting speeds.[23)] Both Heckel analysis and the SRS index are commonly used to evaluate compression properties. For example, inorganic materials such as calcium phosphate and magnesium bicarbonate show low SRS due to fragmentation during compression. In contrast, viscoplastic and viscoelastic materials, such as microcrystalline cellulose and starch, show high SRS. However, it is not easy to compare the data from different studies, as the measurement results depend on the test procedure.[24–26)] The range of tableting speeds for obtaining SRS varies among studies,[23,27–29)] and an appropriate test procedure has not been clarified.

We previously showed that the tableting speed-dependent compressibility properties of API in a powder mixture can be characterized using the out-of-die SRS obtained with a laboratory-scale rotary tablet press as an indicator for samples different excipients compositions and an API concentration of 20% (w/w).[30)] In this study, we first demonstrated the scale-up applicability of the proposed method. We then determined the effect of the raw material viscoelasticity and API concentration on the out-of-die SRS.

Results and Discussion

Comparison of In-Die and Out-of-Die Methods Sample compressibility was evaluated by the in-die and out-of-die Heckel analyses. The mean yield pressure ($P_{y,in}$) was obtained through the linear approximation of the data in the compression pressure range of 50–120 MPa in the out-of-die Heckel plot of the tablets manufactured in the weight range of 200 ± 2 mg. Similarly, The mean yield pressure ($P_{y,out}$) was obtained *via* linear approximation of 3–5 data points in the pressure range of 98–290 MPa in the out-of-die Heckel plot of data for tablets manufactured in the same weight range using the least-squares method. The results showed that the slope of the linear part in the in-die Heckel plot was similar for all samples and was independent of the tableting speed. In contrast, in the out-of-die Heckel plot, the linear part of the slope decreased with the tableting speed only for ibuprofen 20% (w/w) powder (Figs. 1, 2). Table 1 shows the mean yield pressures of the placebo, cilostazol 20% (w/w) powder, and ibuprofen 20% (w/w) powder groups measured by the in-die and out-of-die methods. $P_{y,out}$ was higher than $P_{y,in}$ for all samples. The ratio of $P_{y,out}$ to $P_{y,in}$ was approximately 1.4-fold for the placebo and cilostazol 20% (w/w) powder and 1.9 to 3.8-fold for ibuprofen 20% (w/w) powder, showing a remarkable difference depending on the peripheral speed. In-die Heckel analysis is a simple procedure for a small amount of powder, and has been widely used to evaluate the compaction properties of powders. Our previous study showed that SRS based on out-of-die Heckel plots using a laboratory-scale rotary tablet press is useful as an index for detecting the compression properties of APIs even in cases with different excipient compositions.[30)] As shown in Table 2, the capping tendency became more pronounced with increasing tableting speed. Therefore, evaluation by the out-of-die

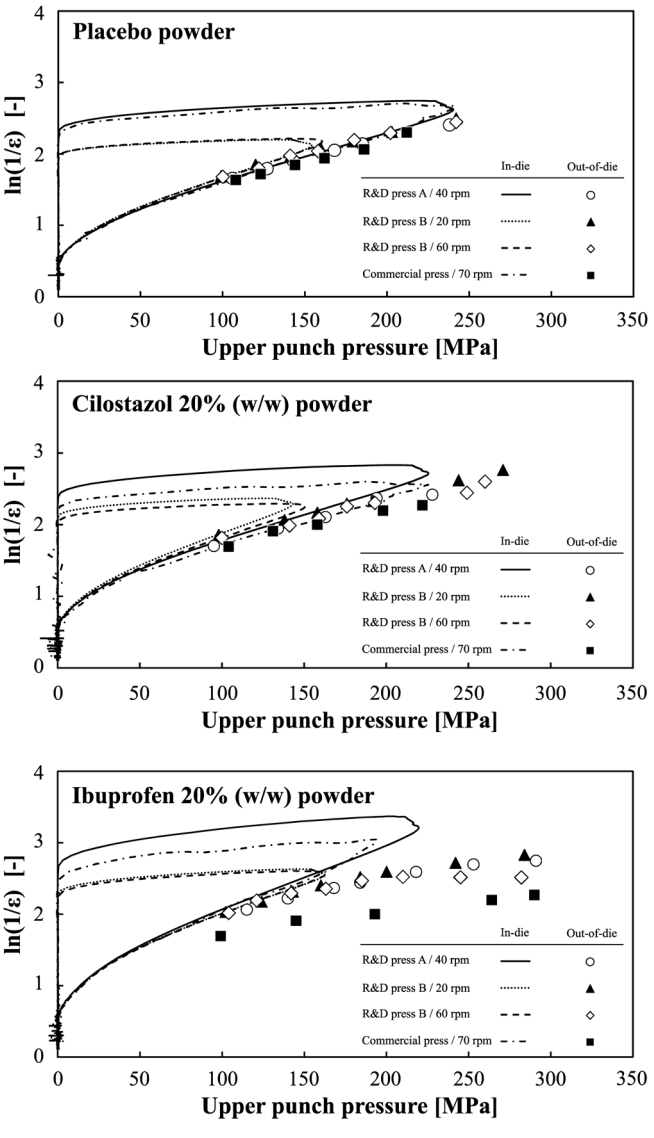

Fig. 1. Typical In-Die and Out-of-Die Heckel Plots

SRS using the laboratory-scale rotary tablet press is considered to accurately reflect commercial-scale. It has been used to classify the deformation properties of powders during the compression, using single components of API and excipients and pharmaceutical formulations.[19,31,32] However, for in-die Heckel analysis, the mean yield pressure varies with the range of compression pressures to be linearly approximated, and the mean yield pressure is affected by the weight and true density of the sample.[24] In contrast, it is obviously that $P_{y,in}$ is significantly lower than $P_{y,out}$ because of elasticity properties.[33] As shown in Fig. 3, the ER_{out} was more significant than the ER_{in} in the elastic recovery, suggesting that the difference in the mean yield pressure was due to elastic recovery. However, the ER_{out} of the tablets manufactured under the peripheral speed conditions of the laboratory-scale and commercial-scale rotary tablet presses differed only for cilostazol 20% (w/w) powder but not for the placebo and ibuprofen 20% (w/w) powder, and there was no correlation with the capping tendency. Thus, although in-die Heckel analysis is simple, it is essential to precisely measure the punch displacement and force after correcting for the effect of elastic deformation of the machine. In addition, it does not include the effect of elastic recovery of the tablet ejected from the tablet press, making this approach unsuitable for characterizing API properties from powder mixture as in this study. Therefore, because the in-die analysis has limited utility compared to raw material properties, out-of-die analysis is considered more practical.

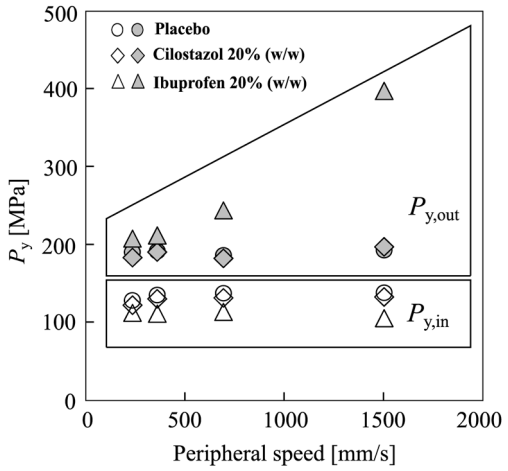

Fig. 2. Relationship between Mean Yield Pressure Obtained from In-Die (Open Symbol) or Out-of-Die (Closed Symbol) Heckel Analysis, and Peripheral Speeds

Appropriate Conditions for Obtaining Out-of-Die SRS In a previous study, the in-die SRS was used to demonstrate the relationship between the deformation properties of two grades of paracetamol and 11 pharmaceutical excipients with different particle sizes.[34] However, as the difference between the two tableting speeds increased, the SRS index became more sensitive, although the appropriate experimental conditions have not been clarified. The available turret rotation speed of a rotary tablet press depends on the model and press size. In the present study, to obtain the out-of-die SRS, $P_{y1,out}$, and $P_{y2,out}$, experiments with low and high tableting speeds feasible on a rotary tablet press were used. As shown in Table 3, the peripheral speed varied greatly depending on the scale of the rotary tablet press and tableting conditions. Table 4 shows the in-die SRS and out-of-die SRS obtained from $P_{y,in}$ and $P_{y,out}$ from two data sets with different tableting speeds to quantitatively evaluate the effect of tableting speed. Both the placebo and cilostazol 20% (w/w) powder, without capping tendency, and ibuprofen 20% (w/w) powder, with capping tendency, showed a low in-die SRS of $<8.1\%$. In contrast, the out-of-die SRS was similar to the in-die SRS for the placebo and cilostazol 20% (w/w) powder, but for ibuprofen 20% (w/w) powder, the out-of-die SRS was higher than the in-die SRS under all but one experimental condition. Besides, the capping tendency increased under the commercial-scale rotary tablet press conditions, confirming the scale-up extrapolation. Figure 4 shows the relationship between the peripheral speed difference and out-of-die SRS found in this study. A higher out-of-die SRS was observed as the peripheral speed difference increased. The peripheral speed difference required to characterize the API-dependent deformation behavior from the powder mixture containing cilostazol and ibuprofen was more than 300 mm/s. This test condition was achieved by manufacturing tablets using the laboratory-scale rotary tablet press B with turret rotation speeds of 20 and 60 rpm.

Evaluation of Viscoelasticity Based on Stress Relaxation Test A stress relaxation test was performed to evaluate the

Table 1. In-Die and Out-of-Die Heckel Analysis Results

Sample	Peripheral speed [mm/s]	In-die				Out-of-die			
		K [1/MPa]	A [—]	R^2	$P_{y,in}$ [MPa]	K [1/MPa]	A [—]	R^2	$P_{y,out}$ [MPa]
Placebo powder	230	0.0079	0.8737	0.999	126.5	0.0053	1.2198	0.999	188.3
	356	0.0075	0.8915	0.999	133.4	0.0053	1.1553	0.998	189.5
	691	0.0074	0.8772	0.999	135.8	0.0054	1.2031	0.989	184.3
	1503	0.0073	0.8628	0.997	136.3	0.0052	1.0919	1.000	191.0
Cilostazol 20% (w/w) powder	230	0.0083	1.0191	0.998	120.5	0.0055	1.3502	0.991	181.6
	356	0.0078	1.0084	0.999	128.7	0.0053	1.2565	0.932	188.5
	691	0.0077	1.0108	0.998	129.8	0.0055	1.0724	0.962	180.5
	1503	0.0076	0.9412	0.999	131.1	0.0051	1.3310	0.991	195.2
Ibuprofen 20% (w/w) powder	230	0.0090	1.1003	0.998	110.7	0.0049	1.6248	0.999	205.9
	356	0.0091	1.1522	0.999	109.4	0.0048	1.5591	0.990	209.8
	691	0.0089	1.0844	0.998	111.9	0.0041	1.6983	0.978	242.1
	1503	0.0096	1.0794	0.985	103.8	0.0025	1.5447	0.994	395.1

Data for peripheral speeds 230 and 691 mm/s in the in-die Heckel analysis are mean of $n = 3$, and other data are mean of $n = 5$.

Table 2. Tablet Capping Tendency

Rotary tablet press	Peripheral speed [mm/s]	The number of capping [counts]					
		Placebo powder		Cilostazol 20% (w/w) powder		Ibuprofen 20% (w/w) powder	
		One-side	Both side	One-side	Both side	One-side	Both side
Laboratory-scale rotary press A	356	No capping		No capping		No capping	
Laboratory-scale rotary press B	230	No capping		No capping		No capping	
	691	No capping		No capping		16[a)]	0[a)]
Commercial-scale rotary press	1503	No capping		No capping		13[a)]	7[a)]

a) Number of capping in 20 tablets.

Table 3. Types of Rotary Tablet Press and Pitch Circle Diameter, and Process Parameters Related to Tableting Speed

Rotary tablet press		Turret rotation speed	Peripheral speed	Dwell time
Scale and type of rotary tablet press	PCD [mm]	[rpm]	[mm/s]	[ms]
Laboratory-scale rotary press A	170	40	356	35
Laboratory-scale rotary press B	220	20/60	230/691	73/9
Commercial-scale rotary press	410	70	1503	4

PCD: Pitch circle diameter of turret

Table 4. Combination of Peripheral Speed and In-Die and Out-of-Die SRS

Peripheral speed [mm/s]		Placebo powder		Cilostazol 20% (w/w) powder		Ibuprofen 20% (w/w) powder %	
Low	High	SRS_{in} [%]	SRS_{out} [%]	SRS_{in} [%]	SRS_{out} [%]	SRS_{in} [%]	SRS_{out} [%]
230	356	<0	<0	0.0	<0	0.0	<0
356	691	1.8	<0	0.8	<0	2.3	13.3
356	1503	2.2	0.0	1.8	3.5	< 0	46.9
230	691	6.8	<0	7.2	<0	1.1	14.9
230	1503	7.2	1.4	8.1	7.0	<0	47.9
691	1503	0.4	3.5	1.0	7.5	<0	38.7

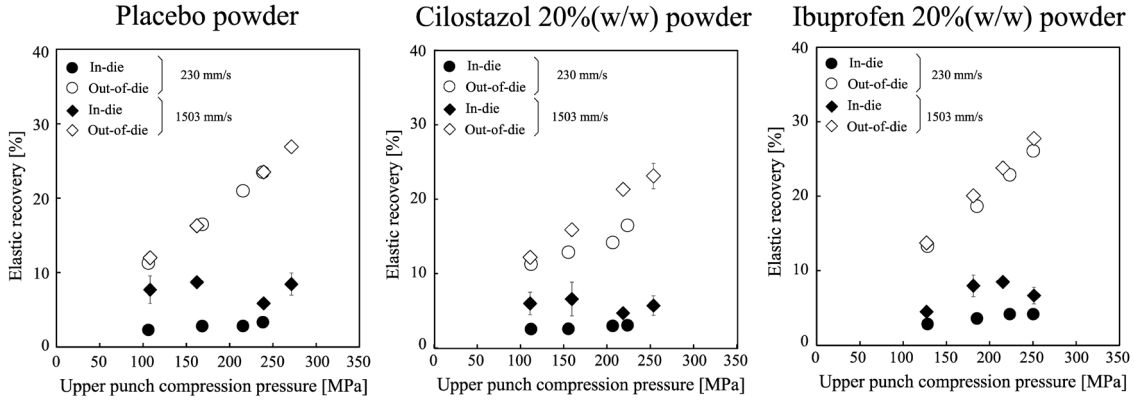

Fig. 3. Relationship between Elastic Recovery as a Function of Compression Pressure and Peripheral Speed
(mean ± S.D., $n = 5$).

viscoelastic properties of cilostazol and ibuprofen. Figure 5 shows the stress relaxation curves obtained at stresses of 40, 80, and 160 MPa. The stress relaxation behavior was analyzed by modeling with a three-element generalized Maxwell model (Table 5). At the same constant stress, the strain was lower for ibuprofen than for the placebo and cilostazol. This corresponds to the poor compressibility of ibuprofen compared to that of the placebo and cilostazol. For the placebo and cilostazol, the viscosity and elasticity coefficients increased with increasing stress/strain during the test. In contrast, the viscosity coefficients of ibuprofen were almost unchanged at all stress levels, whereas the elasticity coefficients increased significantly. Particularly, E_0 was the elasticity coefficient that remained after a long compression time, and was significantly higher than E_1 and E_2. The value of η_1, which corresponds to fast relaxation of the viscosity coefficient, was significantly lower than that of η_2, with a small standard deviation. The relationship between strain, E_0, and η_1 is shown in Fig. 6. The viscoelastic behaviors differed for ibuprofen with capping tendency, cilostazol without capping tendency, and the pla-

cebo. Interestingly, even the ibuprofen with capping tendency showed a significant value for η_2, a delayed viscosity coefficient. The tensile strength of the tablets after the stress relaxation test was similar for the placebo, cilostazol, and ibuprofen, and no capping or lamination was observed for ibuprofen. This may be because of the effect of two factors: compression speed and time. First, the compression speed of the stress relaxation test is 1 mm/s, which is significantly slower than the tableting speed of the rotary tablet press. In addition, the time of the stress relaxation test was 180 s, and the strain was maintained than the tableting process. Therefore, the effect of delayed viscosity improved the compactibility of ibuprofen.

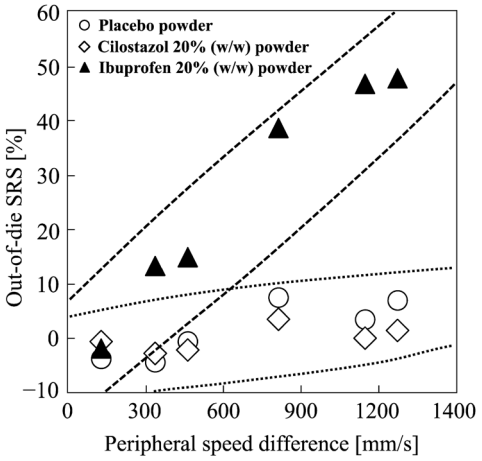

Fig. 4. Dependence of Out-of-Die SRS on Peripheral Speed Difference

The dashed line is the 99% confidence interval for the ibuprofen 20% (w/w) powder data with capping tendencies, and the dotted line is the 99% confidence interval for the placebo and the cilosazol 20% (w/w) powder data without capping tendencies.

Effect of Concentration of APIs in Powder Mixtures on SRS The effects of tableting speed on the compressibility and compactibility of the placebo and samples with different API concentrations were evaluated by Heckel analysis[15] and Ryshkewitch–Duckworth analysis.[35] Figures 7–9 show the Heckel plot (compressibility) and Ryshkewitch–Duckworth plot (compactibility) for the placebo, cilostazol, and ibuprofen. For the placebo, both compressibility and compactibility showed good linearity regardless of the tableting speed (Fig. 7). Similarly, for cilostazol, the Heckel plot and Ryshkewitch–Duckworth plot were linear in the concentration range of 5–40%. In contrast, for ibuprofen, the Heckel plot became non-linear at concentrations above 10% (Fig. 8). In the Ryshkewitch–Duckworth plot, at high tableting speed, ibuprofen 10% (w/w) powder decreased the compressibility in the region of high compression pressure, resulting in decreased compactibility; this tendency became more pronounced for ibuprofen 40% (w/w) powder (Fig. 9). Table 6 shows the compressibility SRS and compactibility SRS. The compressibility SRS was obtained from the mean yield pressure by Heckel analysis, and the compactibility SRS was obtained from the bonding capacity by Ryshkewitch–Duckworth analysis. For the placebo, the compressibility SRS and compactibility SRS were 0.4% and 3.9%, respectively. Thus both compressibility and compactibility-based SRS are dependent on API concentra-

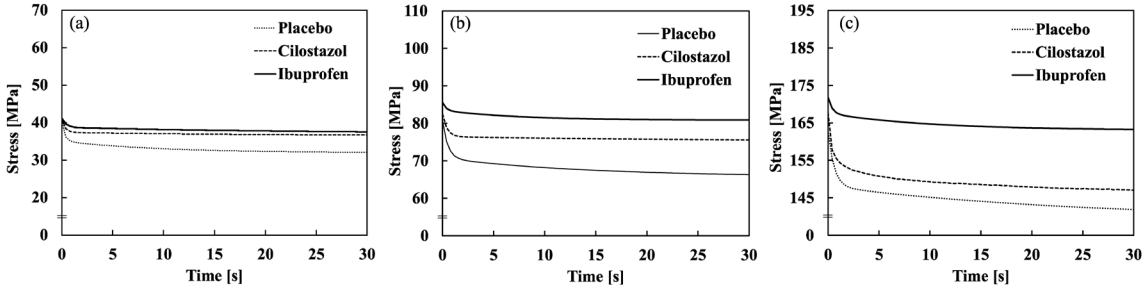

Fig. 5. Stress Relaxation Curves of Placebo and APIs Obtained at Different Stresses

Mean, $n = 3$. (a) 40 MPa, (b) 80 MPa, and (c) 160 MPa.

Table 5. Apparent Elasticity and Viscosity Coefficient of Placebo and APIs

Sample	Stress	Strain	Elasticity coefficient				Viscosity coefficient		
			E_0	E_1	E_2	$\sum_{i=3}^{i} E_i$	η_1	η_2	$\sum_{i=3}^{i} \eta_i$
	[MPa]	[—]	[MPa]	[MPa]	[MPa]	[MPa]	[MPa·s]	[MPa·s]	[MPa·s]
Placebo powder	40	0.267 (0.01)	117.3 (3.9)	21.9 (2.1)	12.2 (0.9)	151.4 (5.2)	6.1 (0.6)	114.9 (5.3)	120.9 (5.2)
	80	0.351 (0.00)	186.6 (2.3)	30.1 (1.6)	14.3 (0.7)	231.0 (2.6)	13.9 (0.8)	192.1 (26.1)	206.0 (26.7)
	160	0.468 (0.02)	307.7 (11.6)	34.4 (2.3)	20.3 (1.5)	362.5 (14.5)	20.8 (2.6)	424.7 (127.5)	445.5 (125.4)
Cilostazol	40	0.256 (0.00)	134.5 (11.7)	17.8 (6.8)	6.3 (4.0)	158.7 (1.2)	5.4 (1.7)	84.3 (23.1)	89.7 (24.8)
	80	0.322 (0.01)	234.6 (3.34)	18.3 (0.9)	5.5 (1.0)	258.4 (3.1)	8.2 (1.1)	121.4 (13.4)	129.5 (13.1)
	160	0.338 (0.01)	430.5 (15.2)	38.8 (10.2)	24.5 (9.2)	493.8 (4.5)	16.1 (3.3)	333.9 (171.2)	350.0 (174.4)
Ibuprofen	40	0.213 (0.01)	176.7 (6.2)	11.7 (0.4)	6.9 (1.1)	195.4 (6.9)	4.9 (0.4)	117.8 (53.0)	122.7 (52.8)
	80	0.252 (0.00)	316.2 (5.3)	8.7 (0.5)	10.5 (0.0)	335.4 (4.8)	2.5 (0.2)	78.3 (1.2)	80.8 (1.0)
	160	0.290 (0.01)	562.2 (16.4)	12.5 (4.4)	14.3 (1.5)	589.0 (20.8)	5.2 (0.6)	160.8 (22.5)	166.1 (22.3)

Mean (S.D.), $n = 3$.

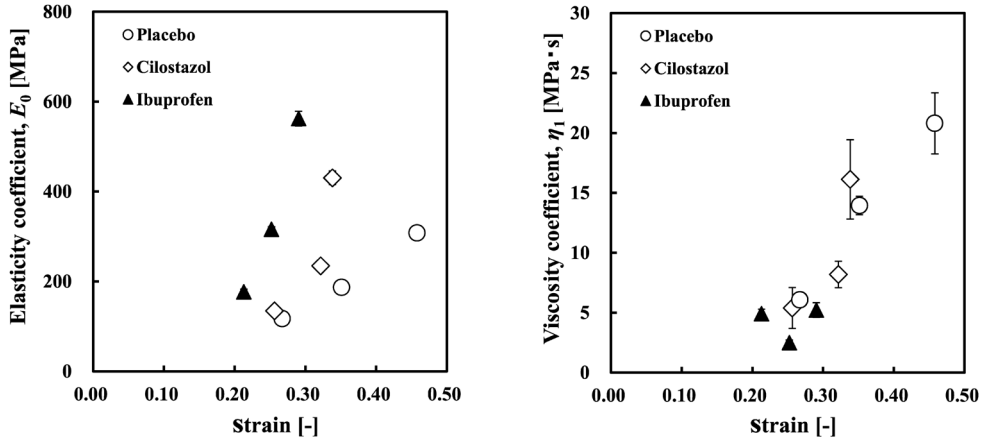

Fig. 6. Relationship between Strain and Apparent Elasticity and Viscosity Coefficients

Mean ± S.D., $n = 3$.

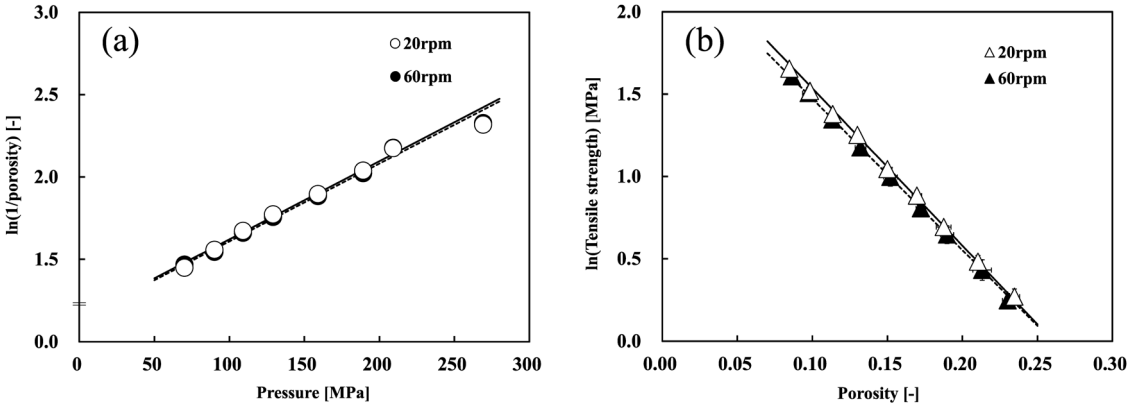

Fig. 7. Effect of Tableting Speed on (a) Compressibility and (b) Compactibility Profiles of Placebo Powder

Mean ± S.D., $n = 5$.

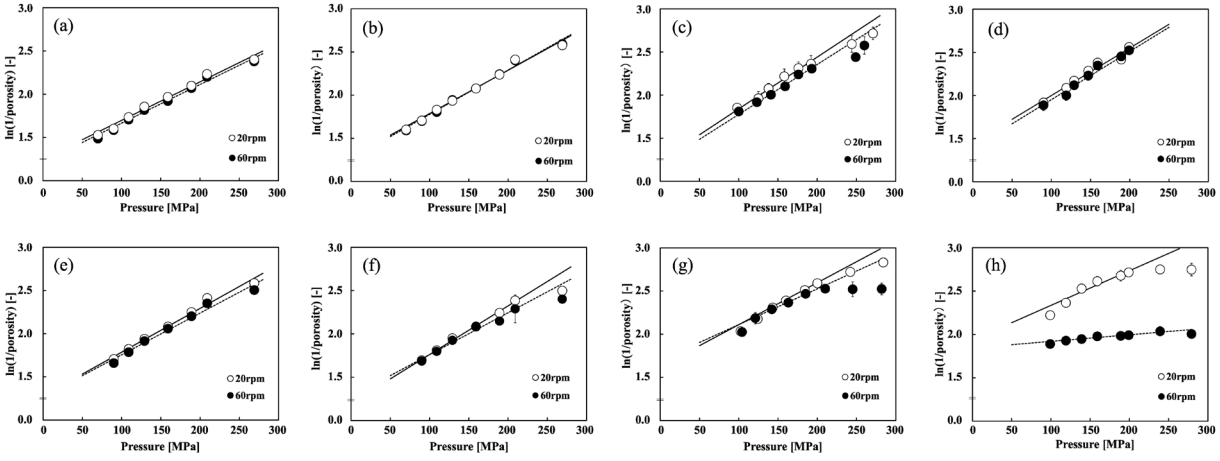

Fig. 8. Comparison of Effect of Tableting Speed on Compressibility Profile of Cilostazol and Ibuprofen Powders

(a), (b), (c) and (d) represent cilostazol concentrations of 5, 10, 2 and 40% (w/w), respectively; (e), (f), (g) and (h) represent compressibility profiles with ibuprofen concentrations of 5, 10, 20 and 40% (w/w), respectively. Mean ± S.D., $n = 10$.

tion. Moreover, the compactibility SRS should be associated when discussing the tablet strengths and fracture properties, such as capping tendency. The compressibility SRS of Cilostazol 5–40% (w/w) powders without capping tendency is up to 3.6%, and the compactibility SRS is up to 14.9%. In contrast, ibuprofen showed capping tendency in powders containing more than 10% (w/w), with the compressibility SRS ranging from 14.0 to 81.0% and the compactibility SRS from 5.8 to 63.7%. Both compressibility SRS and compactibility SRS were higher for the powder containing ibuprofen. In calculating SRS for both compressibility and compactibility, it may be possible to evaluate the capping property and the deformation property of API in the powder mixtures.

Relationship of Viscoelasticity to SRS of API-Containing

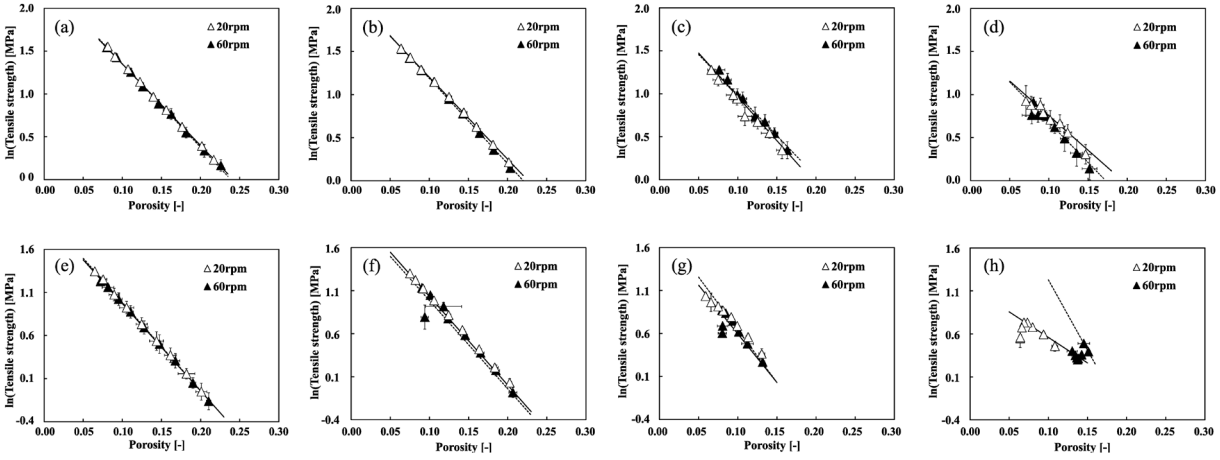

Fig. 9. Comparison of Effect of Tableting Speed on Compactibility Profile of Cilostazol and Ibuprofen Powders

(a), (b), (c) and (d) represent cilostazol concentrations of 5, 10, 20 and 40% (w/w), respectively; (e), (f), (g) and (h) represent compactibility profiles with ibuprofen concentrations of 5, 10, 20 and 40% (w/w), respectively. Mean ± S.D., $n = 10$.

Table 6. Compressibility SRS and Compactibility SRS of Samples Containing Placebo and Different Concentrations of API

	API conc.	Peripheral speed	Compressibility					Compactibility		
			K	A	R^2	P_y	SRS	k	R^2	SRS
	[%(w/w)]	[mm/s]	[1/MPa]	[—]		[MPa]	[%]	[—]		[%]
Placebo powder	—	230	0.00474	1.14780	0.9958	211	0.4	9.54944	0.9989	3.9
		691	0.00472	1.13729	0.9958	212		9.19151	1.0000	
Cilostazol powder	5	230	0.00445	1.25123	0.9819	225	<0.0	9.51741	0.9996	2.3
		691	0.00446	1.22019	0.9876	224		9.74600	0.9987	
	10	230	0.00502	1.28505	0.9829	199	<0.0	9.51274	0.9993	3.9
		691	0.00514	1.26361	0.9867	195		9.89812	0.9987	
	20	230	0.00601	1.23935	0.9742	166	3.6	10.1949	0.9895	7.9
		691	0.00579	1.19721	0.9897	173		9.44685	0.9987	
	40	230	0.00551	1.44835	0.9751	182	<0.0	8.01960	0.9342	14.9
		691	0.00560	1.39077	0.9736	179		9.42801	0.9690	
Ibuprofen powder	5	230	0.00508	1.27697	0.9838	197	4.8	9.99910	0.9997	<0.0
		691	0.00484	1.27143	0.9775	207		10.2493	0.9989	
	10	230	0.00562	1.19931	0.9960	178	14.0	9.95789	0.9995	5.8
		691	0.00484	1.27703	0.9808	207		10.5707	0.9908	
	20	230	0.00486	1.62477	0.9995	206	14.9	9.46055	0.9909	22.8
		691	0.00413	1.69827	0.9781	242		12.2560	0.9874	
	40	230	0.00401	1.93538	0.9266	250	81.0	5.93596	0.9728	63.7
		691	0.00076	1.84364	0.9104	1311		16.3624	1.0000	

Mean, $n = 10$.

Powder Mixture As shown in Table 5, the viscoelastic properties of the placebo, cilostazol, and ibuprofen are characterized by E_0 and η_1. These properties were compared by plotting E_0/η_1 *versus* strain. As shown in Fig. 10, E_0/η_1 did not change significantly with increasing strain in the placebo and cilostazol, whereas E_0/η_1 increased significantly with increasing strain in ibuprofen. As shown in Table 2, the capping tendency was observed only in ibuprofen tablets. Other than the raw material properties, capping is caused by air entrapment during compression. However, based on our viscoelastic evaluation and SRS measurements, capping is likely due to the low viscosity and high elasticity of ibuprofen. In general, the viscosity of solid materials is closely related to plasticity and is rate/time-dependent. Therefore, we considered that the viscoelasticity of ibuprofen appeared as the difference between the SRS of the placebo and cilostazol. Thus, viscoelasticity and viscoplasticity affect SRS; however, a disadvantage of these values is that the difference in deformation modes cannot be identified using conventional methods. Katz and Buckner reported that SRS based on the indentation creep test is less sensitive to the raw material's elastic behavior and particle size.[21] Furthermore, the test does not require a high-speed compression test for evaluation to be performed more quickly than when using conventional methods. Desbois *et al.* proposed a new method to evaluate only viscoelastic behavior during powder compaction using a compaction simulator.[36]

Their method enabled to the measurement of the apparent bulk and shear moduli as a function of the strain rate. The stress relaxation test and out-of-die SRS index are practice tests that can be performed with conventional equipment. Considering the result of Katz and Buckner,[21] Desbois *et al.*,[36] our results reflect both the viscoelastic and viscoplastic behaviors of the raw material, based on the relationship between the elasticity/viscosity ratio and the out-of-die SRS obtained from stress relaxation tests. Our approach is practical because the tableting speed-dependent deformation characteristics specific to APIs can be easily determined by appropriate testing, even for a powder mixture of APIs and excipients. APIs often have poor flowability and compressibility. The incorporation of deformation mode-specific test methods can quantify on the tableting speed-dependent compression properties of APIs.

Conclusion

The effect of tableting speed on the deformation properties of APIs was investigated using placebo powders and powder mixtures containing cilostazol or ibuprofen as a model. We characterized compression properties of APIs in the mixed powder as an index of the out-of-die SRS. The findings of the present study are as follows.

[1] The out-of-die SRS obtained by using a laboratory-scale rotary tablet press could be extrapolated to a commercial scale.

[2] The viscoelasticity of the placebo and API was evaluated, and the effect of tableting speed was more pronounced for ibuprofen, which has high elasticity/low viscosity compared to cilostazol or the placebo, which has low elasticity/high viscosity.

[3] The peripheral speed difference of more than 300 mm/s was required to calculate the out-of-die SRS, which characterizes the deformation properties of cilostazol and ibuprofen in the powder mixture.

[4] The effect of tableting speed on the compressibility was detectable as the out-of-die SRS index when the API concentration was more than 10% (w/w).

In the early formulation development stage, the amount of available APIs is small, and poorly water-soluble drugs are often pulverized, resulting in poor flowability. This is a limitation of the method when evaluating the compression properties of the API alone. In the proposed method, the APIs are mixed with pharmaceutical excipients such as lactose and microcrystalline cellulose to improve API handlings during the testing. This step is also helpful for quantitatively evaluating compression properties depending on the tableting speed by using the out-of-die SRS obtained under appropriate experimental conditions as an indicator.

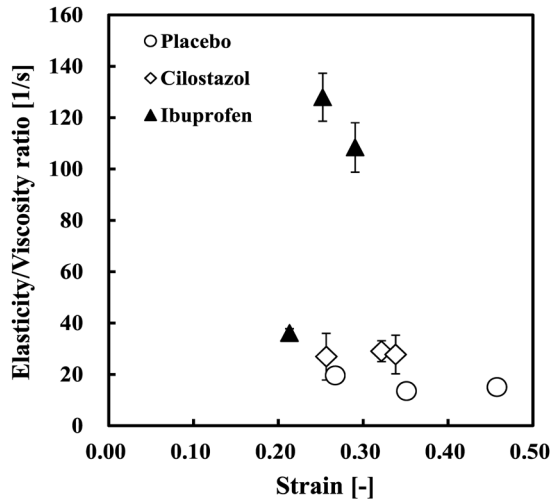

Fig. 10. Relationship between Strain and Elasticity/Viscosity Ratio
Mean ± S.D., $n = 3$.

Experimental

Materials Cilostazol (Otsuka Pharmaceutical, Tokyo, Japan), an antiplatelet agent, and ibuprofen (Hachidai Pharmaceutical, Osaka, Japan), a nonsteroidal anti-inflammatory analgesic, were used as model APIs. Lactose monohydrate (Dilactose S; Freund, Tokyo, Japan), microcrystalline cellulose (Ceolus UF-711; Asahi Kasei, Tokyo, Japan), and vegetable-derived magnesium stearate (Taihei Chemical, Osaka, Japan) were used as excipients. A mixture of lactose monohydrate and microcrystalline cellulose (7 : 3) with 1% (w/w) magnesium stearate was used as the placebo mixture. Cilostazol and ibuprofen were added to the placebo mixture at a concentration of 5, 10, 20, and 40% (w/w) powder.

Powder Mixture Preparation The batch scale of the powder mixture was 1 kg/batch. All raw materials except magnesium stearate were mixed in a polyethylene bag and screened through a 710 μm sieve for de-aggregation. After that, raw materials were charged into a drum blender with a 9 L capacity and mixed at 18 rpm for 30 min. The drum blender was lubricated at 18 rpm for 5 min.

Particle Size Distribution Particle size distributions of APIs and excipients were measured by a laser diffraction scattering method (LDSA-1500 A; Tohnichi Computer Applications, Tokyo, Japan) with a focal length of 100 mm and an

Table 7. True Density and Water Content of Sample

API concentration	Placebo		Cilostazol		Ibuprofen	
	True density	Water Content	True density	Water Content	True density	Water Content
[%(w/w)]	[g/cm^3]	[%]	[g/cm^3]	[%]	[g/cm^3]	[%]
0	1.5565	3.9	—		—	
5			1.5361	4.3	1.5007	4.9
10			1.5009	4.1	1.4971	4.0
20		—	1.4670	3.7	1.4170	4.7
40			1.4230	3.1	1.4170	3.0
100			1.2320	0.07	1.0950	0.14

True density is the mean of $n = 5$. Water content is $n = 1$.

air pressure of 0.05 MPa. The 50% particle size of cilostazol and ibuprofen were 15.5 ± 0.3 and $26.2 \pm 1.6\,\mu$m, respectively (mean ± standard deviation (S.D.), $n = 3$).

True Density True density (ρ_{true}) of the samples was measured by a gas pycnometer (Pentapycnometer PPY-15T; Quantachrome, Boynton Beach, FL, U.S.A.) (Table 7).

Water Content Water content of the samples was measured by the Karl Fischer method (Volumetric moisture meter KF-200; Mitsubishi Chemical Analytech, Japan) (Table 7).

Stress Relaxation Stress relaxation tests were conducted using a compaction analyzer (TabFlex; Okada Seiko, Tokyo, Japan) to evaluate the apparent viscoelasticity of the placebo, cilostazol, and ibuprofen. The accuracies of the displacement and force sensors were $\pm 3.5\,\mu$m and $\pm 0.8\%$, respectively. IPT-B-type punches with a flat face and an 8 mm diameter were used. Before the test, the punches were compressed at low speed in direct contact to obtain a correction equation for machine deformation ($y = 0.0003x^2 + 0.016x - 0.007$, where x and y are the loads and corrected distance between punches, respectively). As the loads applied in the stress relaxation test were 2, 4, and 8 kN, the maximum load at correction was set to 10 kN to cover these ranges. A sample of 200 mg was filled into a die 8 mm diameter and loaded at 1 mm/s. After reaching the maximum load, the constant strain was maintained for 180 s, and the stress and displacement of the punches were measured. The data collection interval was set at 8 ms. At the end of the test, the tablets were ejected to confirm that there was no damage to the tablets. Magnesium stearate was sprayed as a lubricant on the punch faces and die-wall to reduce friction between the tooling and the powder, and excess lubricant was removed. The stress relaxation curves obtained from the experiments were analyzed by the generalized Maxwell model shown in Eq. (1), assuming that the powder is a linear viscoelastic material.[1,14] The Maxwell model is a rheological model in which a spring (elastic component) and dashpot (viscous component) are connected in series to form a single element. In this study, the stress relaxation behavior was expressed using a model with three elements connected in parallel. One of the three elements was used as a spring element only to represent the residual elasticity.

$$\sigma(t) = E_0 \cdot ST + \sum_{i=1}^{n} E_i \cdot e^{-\frac{t}{\tau_i}} \cdot ST \quad (1)$$

The viscosity coefficient is η and is expressed as $\tau = \eta/E$, where ST is strain, E_0 is the instantaneous elastic modulus, Ei and i are the coefficients and terms of the Prony series, and τ is the relaxation time. The stress was almost constant at 60 s after maximum stress was reached. Therefore, E_0, E_1, E_2, η_1, and η_2 were determined to minimize the mean square error of the data and Eq. (1) for the first 60 s of the test.

Compaction Simulator A compaction simulator was used to evaluate the effect of the tableting speed of a commercial-scale rotary tablet press and in-die compression behavior on a commercial-scale rotary tablet press. The STYL'One Evolution (Medelpharm, Beynost, France) is a single-station compaction simulator instrument with a displacement sensor and force sensor that can precisely measure the punch position, punch and ejection forces. The accuracies of the displacement and force sensors were ±0.01 mm and ±0.25 kN, respectively. The motion of the upper and lower punches is ensured by satellite roll screws, and each punch is operated by an independent low-inertia brushless servo motor. These features enable high-precision position control of the punch, and it is possible to simulate the compaction cycle of various rotary tablet presses. The compaction simulator is a helpful tool for reflecting compression behavior to evaluate the effect of the tableting speed on the compaction process. The compaction cycles of two laboratory-scale rotary tablet presses (VELA5 and VIRGO; Kikusui, Kyoto, Japan) and one commercial-scale rotary tablet press (LIBRA; Kikusui) were simulated using the STYL'One Evolution. Table 4 lists the main parameters of each rotary tablet press and simulating turret rotation speed. The data sampling interval of the compaction cycle data per tablet was set to 2 ms. To obtain accurate in-die data, it is necessary to consider the deformation of the machine and punches.[37] Before the experiment, the correction factor for deformation of the machine during compaction was investigated. A flat IPT-B punch (Young's modulus 210 GPa) with a diameter of 8 mm was set, and a load of 20 kN was slowly applied with the upper and lower punches in contact at low speed. Although the distance between the punches was zero, this distance changed slightly as the load was applied. An approximate equation was obtained from the relationship between the load and distance between the punches ($y = -0.00004x^2 + 0.0083x + 0.005$, where x and y are the loads and the corrected distance between punches, respectively).

Tablet Preparation The compaction simulator and conventional laboratory-scale rotary tablet press were used for tableting. For all experiments, IPT-B-type punches with an 8 mm diameter and 15.5 mm radius of the surface curvature were used, and the target tablet weight was 200 mg. As the sample exhibited poor flowability, a force feeder was used to feed the powder into the die. In experiments using the compaction simulator, tablets were manufactured under the four experimental conditions shown in Table 4, with compression pressures ranging from 90 to 270 MPa (up to 290 MPa for some samples) depending on the distance between the upper and lower punches. In contrast, in the experiment using the rotary tablet press (VIRGO), tablets were manufactured by setting the turret rotation speed to 20 or 60 rpm.

Tablet Property Measurements The tablets were stored overnight in an unpackaged condition at 24 °C and <25% relative humidity before evaluating the physical properties. Each tablet weight was measured using an electronic balance (CPA224S; Sartorius, Göttingen, Germany). The tablet thickness was measured using a thickness gauge (ID-C112XBS; Mitutoyo, Kawasaki, Japan). The tablet hardness was determined through the diametrical compression using a tablet hardness tester (MT50; Dr. Schleuniger Pharmatron, Solothurn, Switzerland) at a speed of 0.5 mm/min. The tablet hardness (F) was converted to tensile strength (σ_t) based on Eq. (2). As the tablets had a diameter of 8 mm and the tablet surface had a large radius of curvature, a conversion formula to determine the tensile strength of flat tablets was used.[38]

$$\sigma_t = \frac{2F}{\pi DT} \quad (2)$$

where D is the tablet diameter, and T is the tablet thickness.

The capping tendency was evaluated based on cracking of the tablets during the tablet hardness measurement. In this measurement, a tablet undergoes diametrical compression between two flat platens, generating tensile stress in the tablet

center. A tablet compacted under adequate conditions splits into two pieces from the center, whereas the tablet surface peels off if there is a capping tendency.[39] To quantitatively evaluate the degree of capping tendency, 10 tablets compacted under each manufacturing condition were counted separately for the capping on only one side and the capping on both sides of the tablet surface during the tablet hardness measurement. As the capping on both sides was assumed to be more severe than that on one side, the number of capping occurrences in the two patterns was defined as the capping tendency.

Evaluation of Compressibility Based on Heckel Analysis Compressibility is defined as the relationship between compression pressure and porosity. To evaluate the compressibility, the Heckel equation shown in Eq. (3) was used.[15]

$$\ln\left(\frac{1}{\varepsilon}\right) = KP + A \tag{3}$$

where ε is the porosity of tablet and P is the upper punch compression pressure. The reciprocal of slope (K) of the linear part of the Heckel plot is the mean yield pressure (P_y),[16] where A is the intercept at $p = 0$ when the line of the Heckel plot is extrapolated. Equation (4) was used to calculate the porosity of the tablet.

$$\varepsilon = \frac{\rho_{\text{tablet}}}{\rho_{\text{true}}} \tag{4}$$

In the in-die method, based on the tablet weight and upper and lower punch displacement data obtained from the compaction simulator, the apparent tablet density of powder during the compression ($\rho_{\text{tablet, in-die}}$) was calculated by using Eq. (5).

$$\rho_{\text{tablet,in-die}} = \frac{W_t}{V_u + V_l + S_p D_{\max}} \tag{5}$$

where W_t is the tablet weight, V_u and V_l are the volumes of the cup portion of the upper and lower punches, respectively, and S_p is the surface area of the cylindrical part of the tablet. $D_{\max}$ is the distance between the upper and lower punches at the maximum compression. The punch distance was corrected for the equipment deformation during the compression and each punch force. The compression pressure and the in-die tablet porosity calculated from Eq. (4) were used for the in-die Heckel analysis from Eq. (3). The tablets were manufactured at several compression pressures from 95 to 242 MPa. The least-squares method was used to calculate the slope using data from 50 to 120 MPa of the compression pressure to obtain the mean yield pressure ($P_{y,in}$).

In the out-of-die method, the apparent density of the tablet was calculated from the data of the tablet diameter (D), and thickness (T) ejected from the compaction simulator or rotary tablet press based on Eq. (6).

$$\rho_{\text{tablet,out-of-die}} = \frac{W_t}{\pi(D/2)^2 (T - d_c) + V_u + V_l} \tag{6}$$

where d_c and S_c in Eq. (6) are the cup depth and surface area at the top and bottom of the tablet, respectively, D is the tablet diameter, and T is the tablet thickness. The tablets were manufactured at the compression pressures of 95–291 MPa, with five tablets per point. The porosity of the ejected tablet was calculated from Eqs. (4) and (6). The porosity of the ejected tablet and compression pressure were then used for Heckel analysis. The mean yield pressure ($P_{y,out}$) was obtained based on the data of 4–6 points with compression pressures of 90–210 MPa using the least-squares method.

Evaluation of Compactibility Based on Ryshkewitch–Duckworth Analysis Compactibility, defined as the relationship between porosity and tensile strength, Ryshkewitch–Duckworth analysis using Eq. (7) compactibility.[35]

$$\ln\left(\frac{\sigma_T}{\sigma_0}\right) = -k \cdot \varepsilon \tag{7}$$

where ε is the porosity of tablet, σ_0 is the tensile strength of the material with zero porosity, and k is a constant representing the bonding capacity.[40]

Strain Rate Sensitivity To quantitatively evaluate the effect of tableting speed, the SRS was calculated using P_y obtained from two experiments with different compression speeds based on Eq. (8).[23]

$$\text{SRS} = \frac{P_{y2} - P_{y1}}{P_{y2}} \times 100 \tag{8}$$

P_{y1} was defined as the mean yield pressure at a low tableting speed and P_{y2} was that at a high tableting speed, which was obtained from experiments using the compaction simulator and the rotary tablet press. The in-die and out-of-die methods were defined as in-die SRS and out-of-die SRS, respectively. Additionally, SRS based on compactibility was calculated from the value of slope k of the Ryshkewitch–Duckworth plot for tablets at low and high tableting speeds.

Elastic Recovery Out-of-die elastic recovery (ER_{out}) was calculated using Eq. (9).[41]

$$\text{ER}_{\text{out}} = \frac{H - H_c}{H_c} \times 100 \tag{9}$$

where H is the tablet thickness after ejection and H_c is the powder height in-die at maximum compression. In contrast, in-die elastic recovery (ER_{in}) was calculated using Eq. (10).[42]

$$\text{ER}_{\text{in}} = \frac{H_{\text{zero}} - H_c}{H_c} \times 100 \tag{10}$$

where H_{zero} is the in-die thickness at unloading, which was calculated using data acquisition software.

Definition of Tableting Speed The tableting speed was defined as the peripheral speed rather than the punch velocity.[43] In a typical single-punch press, the punch movement is linear, and the waveform has a saw-tooth shape. In addition, the punch velocity is very slow compared to a rotary tablet press. In contrast, in a rotary tablet press, the punch movement is non-linear and depends on the tablet press model. Therefore, it is difficult to accurately calculate the punch velocity.[44,45] The peripheral speed (v) was calculated using Eq. (11).

$$v = \frac{N}{60} \pi R \tag{11}$$

where N is the turret rotation speed, and R is the pitch circle diameter). Dwell time is defined when the flat part of the punch head moves parallel to the compression rolls in contact with it.[17] In this study, the dwell time was calculated using the data acquisition software. Table 3 shows the pitch circle diameter, turret rotation speed, peripheral speed, and dwell time of the simulated rotary tablet press.

Statistical Analysis JMP13 (SAS Institute Inc., Cary, NC, U.S.A.) was used to analyze the experimental data.

Acknowledgments The experiments using the STYL'One evolution were conducted with the cooperation of Mutual.

Conflict of Interest The authors declare no conflict of interest.

References

1) Casahoursat L., Lemagnen G., Larrouture D., *Drug Dev. Ind. Pharm.*, **14**, 2179–2199 (1988).
2) Nakamura H., Sugino Y., Watano S., *Chem. Pharm. Bull.*, **60**, 772–777 (2012).
3) Celik M., Travers D. N., *Drug Dev. Ind. Pharm.*, **11**, 299–314 (1985).
4) Sugimori K., Mori S., Kawashima Y., *Powder Technol.*, **58**, 259–264 (1989).
5) Sugimori K., Mori S., Kawashima Y., *Chem. Pharm. Bull.*, **37**, 458–462 (1989).
6) Tanino T., Aoki Y., Furuya Y., Sato K., Takeda T., Mizuta T., *Chem. Pharm. Bull.*, **43**, 1772–1779 (1995).
7) Mazel V., Busignies V., Diarra H., Tchoreloff P., *Int. J. Pharm.*, **478**, 702–704 (2015).
8) Ruegger C. E., Çelik M., *Pharm. Dev. Technol.*, **5**, 495–505 (2000).
9) Rippie E. G., Danielson D. W., *J. Pharm. Sci.*, **70**, 476–482 (1981).
10) Danielson D. W., Morehead W. T., Rippie E. G., *J. Pharm. Sci.*, **72**, 342–345 (1983).
11) Al-Ibraheemi Z. A. M., Anuar M. S., Taip F. S., Amin M. C. I., Tahir S. M., Mahdi A. B., *Particul. Sci. Technol.*, **31**, 561–567 (2013).
12) Hiestand E. N., Wells J. E., Peot C. B., Ochs J. F., *J. Pharm. Sci.*, **66**, 510–519 (1977).
13) Roberts R. J., Rowe R. C., *J. Pharm. Pharmacol.*, **52**, 147–150 (2000).
14) Rehula M., Adamek R., Spacek V., *Powder Technol.*, **217**, 510–515 (2012).
15) Heckel R. W., *Trans. Met. Soc. AIME*, **221**, 671–675 (1961).
16) Hersey J. A., Rees J. E., *Nat. Phys. Sci*, **230**, 96 (1971).
17) Leitritz M., Krumme M., Schmidt P. C., *J. Pharm. Pharmacol.*, **48**, 456–462 (2011).
18) Sonnergaard J. M., *Int. J. Pharm.*, **193**, 63–71 (1999).
19) Cespi M., Perinelli D. R., Casettari L., Bonacucina G., Caporicci G., Rendina F., Palmieri G. F., *Int. J. Pharm.*, **477**, 140–147 (2014).
20) ElShaer A., Al-khattawi A., Mohammed A. R., Warzecha M., Lamprou D. A., Hassanin H., *Pharm. Dev. Tech.*, **23**, 442–453 (2018).
21) Katz J. M., Buckner I. S., *J. Pharm. Sci.*, **106**, 843–849 (2017).
22) Hirschberg C., Paul S., Rantanen J., Sun C. C., *Powder Technol.*, **361**, 903–909 (2020).
23) Roberts R. J., Rowe R. C., *J. Pharm. Pharmacol.*, **37**, 377–384 (1985).
24) Gabaude C. M. D., Guillot M., Gautier J. C., Saudemon P., Chulia D., *J. Pharm. Sci.*, **88**, 725–730 (1999).
25) Hooper D., Clarke F., Mitchell J., Snowden M., *J. Nanomed. Nanotechnol.*, **7**, 1–6 (2016).
26) Patel S., Kou X., Hou H. H., Huang Y. B., Strong J. C., Zhang G. G. Z., Sun C. C., *J. Pharm. Sci.*, **106**, 217–223 (2017).
27) Muñoz-Ruiz A., Paronen P., *J. Pharm. Pharmacol.*, **48**, 790–797 (1996).
28) Monedero Perales M. D. C., Muñoz Ruiz A., Velasco Antequera M. V., Jiménez-Castellanos Ballesteros M. R., *Int. J. Pharm.*, **132**, 183–188 (1996).
29) Rojas J., Uribe Y., Zuluaga A., *Pharmazie*, **67**, 513–517 (2012).
30) Mizunaga D., Koseki M., Watano S., *J. Soc. Powder Technol. Japan*, **57**, 577–587 (2020).
31) Tatavarti A. S., Muller F. X., Hoag S. W., *Int. J. Pharm.*, **348**, 46–53 (2008).
32) Tarlier N., Soulairol I., Sanchez-Ballester N., Baylac G., Aubert A., Lefevre P., Bataille B., Sharkawi T., *Int. J. Pharm.*, **547**, 142–149 (2018).
33) Sun C., Grant D. J. W., *Pharm. Dev. Technol.*, **6**, 193–200 (2001).
34) Roberts R. J., Rowe R. C., *J. Pharm. Pharmacol.*, **38**, 567–571 (1986).
35) Ryshkewitch E., *J. Am. Ceram. Soc.*, **36**, 65–68 (1953).
36) Desbois L., Tchoreloff P., Mazel V., *Int. J. Pharm.*, **587**, 119695 (2020).
37) Matz C., Bauer-Brandl A., Rigassi T., Schubert R., Becker D., *Drug Dev. Ind. Pharm.*, **25**, 117–130 (1999).
38) Fell J. T., Newton J. M., *J. Pharm. Sci.*, **59**, 688–691 (1970).
39) Furukawa R., Chen Y., Horiguchi A., Takagaki K., Nishi J., Konishi A., Shirakawa Y., Sugimoto M., Narisawa S., *Int. J. Pharm.*, **493**, 182–191 (2015).
40) Steendam R., Lerk C. F., *Int. J. Pharm.*, **175**, 33–46 (1998).
41) Armstrong N. A., Haines-Nutt R. F., *Powder Technol.*, **9**, 287–290 (1974).
42) Keizer H. L., Kleinebudde P., *Int. J. Pharm.*, **573**, 118810 (2020).
43) Takahashi T., Toyota H., Kuroiwa Y., Kondo H., Dohi M., Hakomori T., Nakamura M., Takeuchi H., *Int. J. Pharm.*, **587**, 119574 (2020).
44) Muller F. X., Augsburger L. L., *J. Pharm. Pharmacol.*, **46**, 468–475 (1994).
45) Kiekens F., Debunne A., Vervaet C., Baert L., Vanhoutte F., Van Assche I., Menard F., Remon J. P., *Eur. J. Pharm. Sci.*, **22**, 117–126 (2004).